

# Cooperative Multi-Agent Assignment over Stochastic Graphs via Constrained Reinforcement Learning

Leopoldo Agorio, Sean Van Alen, Santiago Paternain, Miguel Calvo-Fullana, and Juan Andres Bazerque

**Abstract**—Constrained multi-agent reinforcement learning offers the framework to design scalable and almost surely feasible solutions for teams of agents operating in dynamic environments to carry out conflicting tasks. We address the challenges of multi-agent coordination through an unconventional formulation in which the dual variables are not driven to convergence but are free to cycle, enabling agents to adapt their policies dynamically based on real-time constraint satisfaction levels. The coordination relies on a light single-bit communication protocol over a network with stochastic connectivity. Using this gossiped information, agents update local estimates of the dual variables. Furthermore, we modify the local dual dynamics by introducing a contraction factor, which lets us use finite communication buffers and keep the estimation error bounded. Under this model, we provide theoretical guarantees of almost sure feasibility and corroborate them with numerical experiments in which a team of robots successfully patrols multiple regions, communicating under a time-varying ad-hoc network.

## I. INTRODUCTION

Reinforcement Learning (RL) has emerged as an essential paradigm in artificial intelligence, driven by its ability to learn optimal behaviors through interactions with the environment. In many real-world scenarios, the interactions involve multiple agents with their own objectives, observations, and decision-making processes, giving rise to Multi-Agent Reinforcement Learning (MARL) [1–3]. Centralized solutions—where the set of actions is decided using the full set of observations—struggle to scale with the number of agents, fail to account for individual agent autonomy, and often cannot handle decentralized information structures where agents have limited or private observations [2, 4]. MARL leverages distributed approaches [5]—where each agent has agency over its own decisions based on its own observations—to achieve impressive results in multi-player games, cooperative tasks such as Hanabi [6], emergent behaviors in hide-and-seek environments [7] as

well as real-world applications, such as traffic light control [8], highlighting MARL’s growing potential.

Control applications further highlight MARL’s adaptability, with advances in collision avoidance for autonomous vehicles [9, 10], agile locomotion in legged robots [11, 12], and manipulation in industrial settings [13, 14]. Many of these applications require constrained formulations, where safety [15–17], resource limitations, or task priorities are encoded as mathematical inequalities, giving rise to the critical subfield of Constrained Reinforcement Learning (CRL) [18, 19].

In this work, we focus on multi-agent assignment as a class of MARL problems, in which constraints are essential to model conflicting requirements. Unconstrained multi-agent assignment methods have been proposed, combining reinforcement learning with game theory, having the advantage of minimal [20] or no coordination [21]. However, these works only account for local rewards and do not provide theoretical guarantees that assignment specifications are met. In contrast, we propose a constrained optimization approach to coordinate agents, guaranteeing the satisfaction of global requirements that involve the joint state of all agents.

Therefore, we address the assignment problem under the framework of Constrained Multi-Agent Reinforcement Learning (CMARL) [22–24]. The literature on CMARL addresses challenges such as safe coordination in autonomous fleets [25], fair resource allocation in multi-agent systems [26], and robust cooperation under communication constraints [27]. These constraints may be individually defined per agent [22], or collective, in which all agents are involved in the feasibility of the same constraint [23, 24]. Assignment problems entail multiple such collective constraints but do not admit the aggregate reward structure in [23, 24].

Whether CRL methods are used in scenarios with single or multiple agents, they often employ regularization to reconcile competing objectives, transforming constraints into penalty terms within an aggregate reward function [18, 28]. For instance, a mobile robot navigating crowded environments might balance collision avoidance (a hard constraint) with energy efficiency (a soft objective) by weighting their respective penalties (e.g., [9]). The selection of these weights is non-trivial: overly conservative penalties may lead to overly cautious behavior, while insufficient regularization risks constraint violations [29]. Bayesian methods [30] adapt weights probabilistically, incorporating prior knowledge about constraint

Leopoldo Agorio, Sean Van Allen, and Juan Andres Bazerque are with the Dept. of Electrical and Computer Engineering, Univ. of Pittsburgh, Pittsburgh, PA, USA (emails: lca31@pitt.edu, sgv13@pitt.edu, juanbazerque@pitt.edu).

Santiago Paternain is with the Dept. of Electrical Computer and Systems Engineering, Rensselaer Polytechnic Institute, Troy, NY, USA (e-mail: paters@rpi.edu).

Miguel Calvo-Fullana is with the Dept of Engineering, Universitat Pompeu Fabra, Barcelona, Spain (email: miguel.calvo@upf.edu).

criticality. Heuristic approaches, though less rigorous, remain prevalent in practice, such as reward shaping [31] in which penalties are manually engineered based on domain expertise.

Lagrangian duality [18, 32] provides a principled approach by treating constraints as part of the optimization dual space, dynamically adjusting weights through gradient descent on the dual variables. Even though the duality gap is guaranteed to be zero [32], feasibility is not guaranteed under this approach for problems where the primal maximizer is not unique [33]. In this scenario, both regularization-based and duality methods that rely on the convergence of the multipliers struggle. In particular, the Example 1 in Section II and the discussion in Section III illustrates how regularization fails in assignment problems in which the collective constraints are nonlinear combinations of individual ones.

State augmentation has emerged as a framework to address these limitations by reinterpreting the constrained RL problem through an extended Markov Decision Process (MDP). By treating Lagrangian multipliers as part of the state space, policies gain the ability to condition their actions on both environmental observations and current constraint satisfaction levels [33]. This approach allows for a family of policies that can alternate in order to fulfill tasks while the Lagrangian weights cycle to multiplex between policies. That is, as one policy focuses on attending to one of the several conflicting requirements, Lagrangian weights will evolve as part of the augmented MDP to eventually force a policy shift towards one that tackles another requirement that is not being satisfied. Theoretical analyses show that such approaches preserve convergence guarantees under mild assumptions, effectively converting constrained optimization into an unconstrained problem over the augmented state-action space [34].

In our preliminary work [35], we leverage these extended MDPs to provide multiple agents with the capability of solving assignment problems collaboratively via CMARL. With standard dual methods proving inadequate for such problems, the cycling trajectories of the multipliers in the augmented state drive agents to alternate between tasks. These multipliers are shared among agents through a communication network, enabling coordination without direct access to other agents' states, yielding a distributed protocol that addresses the challenges of multi-agent assignment problems with theoretical feasibility and convergence guarantees. Building on this foundation, we introduce a key novelty in this work: the integration of a gossiping framework [36] to share multipliers across a stochastic communication network [37, 38] established by the agents. This network is inherently dynamic and may even be disconnected across time, reflecting communication ad-hoc conditions frequently found in practice. To address these challenges while maintaining feasibility guarantees, we propose a novel algorithm featuring a contractive update for the augmented multipliers, which lets us use finite communication buffers and keep the estimation error bounded. This innovation enhances scalability and ensures almost sure feasibility in stochastic environments. Leveraging this framework, we prove almost sure feasibility up to an error margin that can be made arbitrarily small, employing a novel proof technique that explicitly accounts for the stochasticity of the communica-

tion graph. We validate our theoretical contributions through extensive numerical experiments, demonstrating the practical applicability of our approach. In these experiments, a team of five robots successfully learns to patrol six regions of interest, showcasing the effectiveness of our algorithm in achieving coordination under realistic communication constraints.

The rest of this paper is organized as follows: In Section II, we introduce multi-agent assignment, formulating it as a feasibility problem and presenting the stochastic graph model that governs agent communication. This model captures the dynamic and potentially disconnected nature of typical networks found in practice, setting the stage for our solution. Section III details the state augmentation approach, which enables agents to coordinate using dual variables shared through the network. We outline the offline training and online execution algorithms, providing the foundation for our distributed multi-agent system. In Section IV, we state and formalize the main theoretical result: almost sure feasibility of the proposed algorithm under mild assumptions. Section V validates our approach through numerical simulations, where a team of five robots successfully patrols six regions of interest, demonstrating consistent feasibility across all runs. Finally, Section VI presents the conclusions, followed by supporting lemmas in the Appendix.

## II. PROBLEM FORMULATION

Consider  $N$  agents interacting with an environment that is modeled as an MDP with transition probabilities  $\mathbb{P}(S_{t+1} | S_t, A_t)$ . For each time index  $t = 0, 1, 2, \dots$ , random variables  $S_t = (S_t^1, \dots, S_t^N)$  and  $A_t = (A_t^1, \dots, A_t^N)$  collect the states  $S_t^n \in \mathcal{S}$  and actions  $A_t^n \in \mathcal{A}$  for all agents. The team receives a vector of rewards  $r(S_t) \in \mathbb{R}^M$  associated with  $M$  different tasks that must be collectively satisfied. We consider a family of assignment problems in which the agents must persistently cover  $M$  regions of the state space denoted by  $\mathcal{S}_m \subset \mathcal{S}$  with  $m = 1, \dots, M$ . Thus, each reward is given by

$$(r(S_t))_m = \max_{n=1, \dots, N} \mathbb{1}[S_t^n \in \mathcal{S}_m], \quad (1)$$

where  $(r)_m$  represents the  $m$ -th element of vector  $r$ , with the index function defined as  $\mathbb{1}[S_t^n \in \mathcal{S}_m] = 1$  if  $S_t^n \in \mathcal{S}_m$  and zero otherwise. Each region  $\mathcal{S}_m$  must be covered by the agents a fraction of the time. Hence, we set the requirements as a vector  $c \in [0, 1]^M$  of  $M$  thresholds on the average rewards, and formulate a Markov decision problem with constraints

$$V(\pi) := \lim_{T \rightarrow \infty} \frac{1}{T} \mathbb{E}_{S_t, A_t \sim \pi} \left[ \sum_{t=0}^{T-1} r(S_t) \right] \geq c, \quad (2)$$

with the inequality being component-wise. The expectation is taken over the transition probabilities and the probability distribution defining the control policy  $\pi(A_t | S_t)$  of the actions of all agents given their states.

A task reward can be incorporated to establish an optimization objective. This can be useful to set a secondary goal, such as minimizing energy consumption in a multi-robot application like the one presented in Example 1 below. However, in the following, we will set the objective to zero and focus on our primary goal of satisfying the specifications.

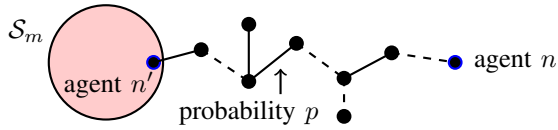


Fig. 1: Agent  $n$  must receive the information that agent  $n'$  is in zone  $S_m$  across the communication graph. Agents  $n \in \mathcal{V} = \{1, \dots, N\}$  are nodes in the stochastic graph  $\mathcal{G}(\mathcal{V}, \mathcal{E}, p)$ , where solid and dashed lines represent the presence or absence of an edge, respectively, at a particular time. If an edge is present, the two nodes connected to the edge can exchange information. Otherwise, the two neighboring agents must wait for a future time in which the edge is present.

Hence, the feasibility problem we aim to solve is

$$P^* = \max_{\pi} 0 \quad (3)$$

$$\text{s. to } \lim_{T \rightarrow \infty} \frac{1}{T} \mathbb{E}_{S_t, A_t \sim \pi} \left[ \sum_{t=0}^{T-1} r(S_t) \right] \geq c.$$

To illustrate the practical use of this problem formulation, we include the following example, which we will explore further in the experiments of Section V.

**Example 1.** Consider a team of  $N$  robots that is required to monitor  $M > N$  areas, visiting areas  $S_1, \dots, S_M$  during fractions of time given by  $c \in [0, 1]^M$ . These conflicting requirements may not be achievable by a single robot, particularly when the aggregate thresholds are greater than one, i.e.,  $\|c\|_1 > 1$ , and not even by multiple robots acting independently following the same optimal single-agent policy. Coordination is thus essential, for which robots can form an ad-hoc communication network.

We aim to solve (3) in a coordinated distributed fashion, in a scenario in which agents do not have access to the whole system state but can only observe their own state  $S_t^n$ . Once deployed, agents will not share their locations. Instead, we will develop a light gossip protocol for agents to exchange *single-bit messages* with their neighbors (Section III-B) over an ad-hoc communication network adhering to the stochastic graph model in [38]. This graph model considers a time domain  $\mathcal{T} \subset \mathbb{N}$  and a set of nodes  $\mathcal{V} = \{1, \dots, N\}$  representing the agents. Then,  $\mathcal{G} = \mathcal{G}(\mathcal{V}, \mathcal{E}, \mathcal{T}, w_G)$  defines a stochastic graph where edges are sampled from a static underlying graph  $G = (\mathcal{V}, \mathcal{E})$ . This *footprint graph*  $G$  indicates pairs of agents that could have connectivity at some point in time. In this model,  $G$  is assumed to be connected, but it is noteworthy that this does not necessarily imply that  $\mathcal{G}$  is connected. Indeed,  $\mathcal{G}$  could be disconnected at all times. Accordingly, the *presence function*  $w_G : \mathcal{E} \times \mathcal{T} \rightarrow \{0, 1\}$  is included to indicate if an edge is present at a given time. We will consider a probabilistic model in which the presence of an edge  $e^{(n, n')} \in \mathcal{E}$  between two agents  $n, n' \in \mathcal{V}$  at time  $t$  is modeled as a Bernoulli random variable with probability  $p$ , i.e.,

$$w_G(n, n', t) \text{ are i.i.d. Bernoulli}(p). \quad (4)$$

Edges are independent of each other, as it is also the activation of an edge across time. Figure 1 illustrates the communication graph for the monitoring problem in Example 1.

### III. OFFLINE TRAINING AND ONLINE EXECUTION

This section presents two algorithms for training the policy and carrying out the tasks. Combined, they solve the CRL problem (3) in the dual domain [32].

Define the Lagrangian associated with problem (3)

$$\mathcal{L}(\pi, \lambda) = \lim_{T \rightarrow \infty} \frac{1}{T} \mathbb{E}_{S_t, A_t \sim \pi} \left[ \sum_{t=0}^{T-1} \lambda^\top (r(S_t) - c) \right], \quad (5)$$

where  $\lambda \in \mathbb{R}_+^M$  denote the dual variables. To obtain the dual, we maximize the Lagrangian in (5). However, we must divert from standard primal-dual algorithms [39] that aim for a dual-optimal vector of multipliers. That is because, under the reward structure of (1), the primal maximizer of (5) for the optimal multipliers does not guarantee a feasible policy for (3). Indeed, the smallest  $M - N + 1$  dual-optimal multipliers must be equal to each other because—as we prove in Lemma 1—otherwise agents only satisfy the  $N$  constraints with highest weighted rewards, leaving the other  $M - N$  unattended. But with  $M - N + 1$  multipliers being equal, the corresponding constraints are indistinguishable when maximizing (5) since any policy followed by the agents with respect to these constraints receives the same weighted reward. For instance, any infeasible policy in which the state of the agents satisfies a single of these  $N - M + 1$  constraints will be a primal maximizer of (5). Even a policy in which the agents' states wander erratically across the regions with equal multipliers, without satisfying any of the  $N - M + 1$  constraints, will maximize (5).

The existence of multiple primal maximizers for the optimal dual prevents the convergence of primal-dual algorithms. Indeed, even if we are given the optimal multiplier, when computing the maximization with respect to the primal variable will recover one of the maximizers which as discussed earlier may not be feasible. This limitation of primal-dual methods is not specific to our problem formulation but was demonstrated in [33] and appears even in convex optimization problems when the Lagrangian is not strictly convex, in which case iterates need to be averaged to achieve convergence [40]. However, we cannot rely on averaging for our assignment problem (3) since the argument for dual optimality of the averaged multipliers relies on the convexity of the primal.

In our constrained RL scenario, we aim to solve problem (3) by an alternative two-step process. First, in an offline training stage, we obtain a policy that optimizes the Lagrangian in (5) for all  $\lambda$ . In the deployment stage, we apply a stochastic dual gradient descent iteration, which causes cycles in  $\lambda$ , and let the agents choose a different policy per rollout, thus preventing an infeasible policy resulting from convergence of  $\lambda$  to the set of optimal multipliers. As multipliers cycle, the rewards in (5) are reweighted, the highest entries of  $\lambda$  alternate, and thus the policy maximizing (5) gives priority to constraints that have not being attended in previous cycles.

Before describing these two stages in more detail, we introduce the following two practical considerations into our design. First, to prevent agents from requiring a full observation of the global  $S_t$  and shield our policy from the exponential growth of the state space, we introduce the following structure

$\pi(A_t|S_t, \lambda^1, \dots, \lambda^N) = \prod_{n=1}^N \pi^n(A_t^n|S_t^n, \lambda^n)$ , in which each agent decides its action taking into account its state  $S_t^n$  and local copies  $\lambda^n$  of  $\lambda$  only.

Note that even if the policies are local, the agents are still coupled by their dynamics and joint rewards. Therefore, the agents still need to optimize the Lagrangian (5) jointly, i.e.,

$$\pi^*[\lambda, \dots, \lambda] = \operatorname{argmax}_{\pi[\lambda, \dots, \lambda]} \lim_{T \rightarrow \infty} \frac{1}{T} \mathbb{E}_{S_t, A_t \sim \pi} \left[ \sum_{t=0}^{T-1} r_\lambda(S_t) \right], \quad (6)$$

in which we reduced notation by optimizing over the global policy  $\pi[\lambda, \dots, \lambda]$  defined as

$$\pi[\lambda, \dots, \lambda](A_t|S_t) := \pi(A_t|S_t, \lambda, \dots, \lambda) \quad (7)$$

$$= \prod_{n=1}^N \pi^n(A_t^n|S_t^n, \lambda), \quad (8)$$

and simplified (5) by defining the following weighted reward

$$r_\lambda(S_t) := \lambda^\top (r(S_t) - c). \quad (9)$$

Furthermore, we parameterize each agent's policy by a vector  $\theta^n \in \mathbb{R}^{p_n}$ . A judicious parameterization will allow us to deal with the augmented state-space  $\mathcal{S} \times \mathbb{R}_+^M$ , containing elements  $(S_t, \lambda)$ , where at least the multipliers are continuous variables. Hence, each agent's action is drawn from a distribution  $\pi_{\theta^n}(A_t^n | S_t^n, \lambda)$ , so that the joint probability distribution with parameters  $\theta = (\theta^1, \dots, \theta^N)$  is

$$\pi_\theta[\lambda, \dots, \lambda](A_t | S_t) := \pi_\theta(A_t | S_t, \lambda, \dots, \lambda) \quad (10)$$

$$= \prod_{n=1}^N \pi_{\theta^n}(A_t^n | S_t^n, \lambda). \quad (11)$$

Next, we describe how to train for these parameters  $\theta$ .

### A. Offline Training

The policy structure in (10) induces a simplified form of the policy gradient [41] that we will use for training. Before presenting this result in Proposition 1, we define the following key concepts. The occupancy measure for the joint state and actions of all agents is given by  $\rho_{\theta, \lambda}(s, a) = \lim_{t \rightarrow \infty} \frac{1}{t} \sum_{\tau=0}^t \mathbb{P}(S_\tau = s) \pi(a|s)$ . Likewise, the state-action value function is defined by  $Q_{\pi_\theta}(s, a, \lambda) = \sum_{t=0}^{\infty} \mathbb{E}_{S_t, A_t \sim \pi_\theta} [r_\lambda(S_t) - \mathcal{L}(\pi_\theta, \lambda) | S_0 = s, A_0 = a]$ , where  $r_\lambda(S_t)$  and  $\mathcal{L}(\pi_\theta, \lambda)$  are the functions defined in (9) and (5), respectively. We further define the state-action value function for agent  $n$  as

$$Q_{\pi_\theta}^n(s, a, \lambda) = \mathbb{E}_{(S_t, A_t)} [Q_{\pi_\theta}(S_t, A_t, \lambda) | S_t^n = s, A_t^n = a]. \quad (12)$$

with expectation over  $(S_t, A_t)$  with probability  $\rho_{\theta, \lambda}(S_t, A_t)$ .

From the perspective of agent  $n$ , the local Q-function (12) is the average of the expected return, assuming that all other agents follow the policy  $\pi_\theta[\lambda, \dots, \lambda]$ . Therefore,  $Q_{\pi_\theta}^n(S_t, A_t, \lambda)$  can be estimated per agent by averaging the global rewards that result from their local states and actions, or modeled as a parametric function of these local entries. The following proposition formalizes these insights, providing

a specific form for the policy gradient Theorem under the separable policy design.

**Proposition 1.** *Assume that the policy of each agent is parameterized by a vector  $\theta^n \in \mathbb{R}^{p_n}$  and that  $A^n \sim \pi_{\theta^n}(\cdot | S^n, \lambda)$ , where  $S^n$  represents the local state of agent  $n$ . Let  $\mathcal{L}(\pi_\theta, \lambda)$  and  $Q_{\pi_\theta}^n(S^n, A^n, \lambda)$  be the functions defined in (5) and (12) respectively. Then, it follows that  $\nabla_{\theta^n} \mathcal{L}(\pi_\theta, \lambda) = \mathbb{E}_{(S^n, A^n) \sim \rho_{\theta, \lambda}} [\nabla_{\theta^n} \log \pi_{\theta^n}(A^n | S^n, \lambda) Q_{\pi_\theta}^n(S^n, A^n, \lambda)]$ .*

*Proof.* See Appendix A.  $\square$

In practice, Proposition 1 tells us that agent  $n$  can compute *locally* its part of the gradient  $\nabla_{\theta^n} \mathcal{L}(\pi_\theta, \lambda)$ , the part needed to update its own local parameters  $\theta^n$ , by using its local policy  $\pi_{\theta^n}(A_t|S_t, \lambda)$ , the multiplier  $\lambda$ , and the local Q-function in (12) averaging over the state and actions of the other agents. Hence, we leverage this local property of the gradients to optimize a parametric version of (6)

$$\pi_{\theta^*}[\lambda, \dots, \lambda] = \operatorname{argmax}_{\pi_\theta[\lambda, \dots, \lambda]} \mathbb{E}_{S_t, A_t \sim \pi_\theta} \left[ \frac{1}{T_0} \sum_{t=0}^{T_0-1} r_\lambda(S_t, A_t) \right], \quad (13)$$

where we used a slight abuse of notation to write a policy  $\pi_\theta[\lambda, \dots, \lambda]$  complying with (10) as the optimization variable instead of  $\theta$ . Notice that, in addition to the parametric expansion of the policies, we introduced a second variation by removing the limit and adhering to a finite time horizon. This modification is key for the practical implementation of the training algorithm, which is detailed in Algorithm 1. Let us remark that the policy parameters that result from (13) do not depend on  $\lambda$ . The augmented state  $(S_t^n, \lambda)$  is the input of each local policy  $\pi_{\theta^n}$  with parameters  $\theta^n$  as in (10).

The modifications above (parameterization and finite horizon) introduce errors in the approximation of (6). We formalize our assumptions on the errors next. Before doing so, we define the truncated value  $V_{T_0}(\pi)$  which becomes

$$V_P := V_{T_0}(\pi_\theta[\lambda, \dots, \lambda]) := \mathbb{E}_{\pi_\theta} \left[ \frac{1}{T_0} \sum_{t=0}^{T_0-1} r(S_t) \right], \quad (14)$$

under policy parameterization, so that  $V_P$  corresponds to the finite-horizon expected cumulative reward attained by the team when running the structured policy (10) for a particular value of  $\lambda$  common to all agents.

**Assumption 1.** (*Approximation error in training*). *The policy parameterization is dense enough, and the horizon is sufficiently large, i.e., For any  $\epsilon > 0$  there exists  $\beta > 0$  and  $T_0 > 0$ , such that for each policy  $\pi[\lambda, \dots, \lambda]$  in (7) there exists a set of parameters  $\theta$  and associated policy  $\pi_\theta[\lambda, \dots, \lambda]$  in (10) such that the respective values  $V = V(\pi[\lambda, \dots, \lambda])$  and  $V_P = V_{T_0}(\pi_\theta[\lambda, \dots, \lambda])$  defined in (2) and (14), satisfy*

$$\lambda^\top (V - V_P) \leq \beta \|\lambda\| + \epsilon. \quad (15)$$

This assumption is tantamount to a universal approximation property, which is standard, for instance, if the policies are parameterized via neural networks. The term  $\epsilon$  in (15) is introduced to bound the truncation error. This bound is not an assumption actually, but results from the rewards in (1)



**Algorithm 1:** Offline training loop for agent  $n$ 


---

```

1: for  $k = 0, 1, \dots$  do
2:   Sample  $\lambda \in \Lambda \subset \mathbb{R}_+^M$ 
3:   Sample  $S_0^n \sim \mathcal{S}$ 
4:   for  $t = 0, \dots, T_0$  do
5:     Sample  $A_t^n \sim \pi_{\theta^n}(A_t^n | S_t^n, \lambda)$ 
6:     Update  $S_{t+1}$ 
7:     Compute  $r(S_{t+1})$ 
8:   end for
9:   Compute  $\nabla_{\theta^n} \mathcal{L}(\pi_{\theta}, \lambda)$  as in Proposition 1
10:  Update  $\theta^n \leftarrow \theta^n + \eta \nabla_{\theta^n} \mathcal{L}(\pi_{\theta}, \lambda)$ 
11: end for

```

---

being bounded. In addition,  $\epsilon$  can accommodate the limited accuracy in solving (13) that results if running a finite number of optimization iterations.

Training for (13) requires that all agents interact to learn from rewards (9) that are jointly activated via (1). This training phase is designed to run offline, with multiple agents and a common  $\lambda$  drawn randomly at the start of an episode and fixed until the end of it. Once each policy  $\pi_{\theta^n}(A_t^n | S_t^n, \lambda)$  in (13) has been trained, its online execution depends only on the local state  $S_t^n$  of the agent, and a common vector  $\lambda$  which varies as agents enter and exit the zones. Thus, agents must engage in online coordination to concur on the trajectory of  $\lambda$ , as described below.

### B. Online Execution

Following the idea of solving the problem in the dual domain, this section presents an algorithm that approximates gradient descent on the dual domain in the online stage. To be formal define the dual function as  $d(\lambda) := \max_{\pi} \mathcal{L}(\pi, \lambda)$ , with  $\mathcal{L}(\pi, \lambda)$  as in (5). According to Danskin's Theorem [42] the minimization of the dual over  $\lambda \geq 0$ , can be achieved by substituting the constraints evaluated at the optimal policy for the gradient of  $d(\lambda)$  to obtain the dual gradient update  $\lambda_{k+1} = [\lambda_k - \eta (V(\pi[\lambda_k, \dots, \lambda_k]) - c)]_+$ , where  $[\cdot]_+$  denotes the projection on the non-negative orthant.

For a data-driven implementation, we run stochastic gradient descent [43], dropping the expectation and replacing it with reward samples. As we did for training, we also set a finite horizon  $T_0$ . Hence, we use the following stochastic dual update

$$\lambda_{k+1} = \left[ (1 - \alpha)\lambda_k + \frac{\eta}{T_0} \sum_{\tau=kT_0}^{(k+1)T_0-1} (c - r(S_{\tau})) \right]_+, \quad (16)$$

introducing also a contractive factor  $(1 - \alpha)$ , with  $\alpha \in (0, 1)$ , which will be necessary to ensure that the errors induced by the stochastic communication graph do not grow unbounded, as we discuss on the remark at the end of this section.

The stochastic update in (16) can be incorporated into the MDP modeling  $S_t$  to form an augmented dynamical system with state  $(S_t, \lambda_k)$  in two timescales, with  $t$  representing the time step and  $k$  indexing the rollout, which spans  $T_0$  time steps from  $kT_0$  to  $(k+1)T_0 - 1$ .

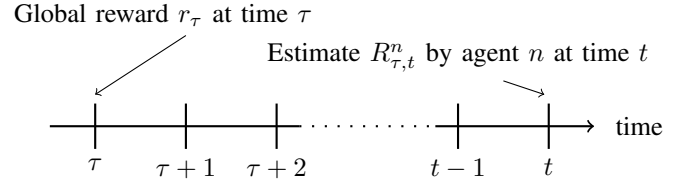


Fig. 2: *Gossip* timeline: Each agent aims to estimate the global vector of rewards  $r(S_{\tau})$ . After  $t - \tau$  time steps, the local estimation of  $r(S_{\tau})$  obtained by agent  $n$  is  $R_{\tau,t}^n$ .

During the execution phase, the agents cannot observe global rewards, which are available locally only to the agents whose states  $S_t^n$  are in regions  $\mathcal{S}_m$ . Hence, the update in (16) is not realizable. Instead, agents exchange the reward information across the communication network to implement (16) in a distributed manner. To devise such a distributed procedure, define  $R_{\tau,t}^n \in \mathbb{R}^M$  as the estimate that the agent  $n$  has at time  $t$  about the actual value of the rewards  $r(S_{\tau})$  at a previous time  $\tau \leq t$ . The communication timeline is shown in Figure 2. Consider an agent  $n'$  whose state  $S_{\tau}^{n'}$  is in region  $\mathcal{S}_m$  at time  $\tau$ . That is  $S_{\tau}^{n'} \in \mathcal{S}_m$  as shown in Figure 1 for the case of our monitoring Example 1. Then agent  $n'$  knows first-hand that the reward for the region  $\mathcal{S}_m$  is being attended at this specific time  $\tau$ , and thus the global reward  $(r(S_{\tau}))_m = 1$  is being attained. Hence, it sets its own local estimate of the reward to one, i.e.,  $(R_{\tau,t}^{n'})_m = (r(S_{\tau}))_m = 1$  for all  $t \geq \tau$ . Then, it passes this information to its neighbors, who will update their local estimates of the reward  $(r(S_{\tau}))_m$  accordingly. Specifically, each agent will receive the local estimates of  $r(S_{\tau})$  from its neighbors and set its local estimate to 1 if any of its neighbors have a local estimate of 1 for the same region. That is equivalent to using the maximum of the local estimates of its neighbors, including itself. In general, the update rule for the local copies of the rewards is given by

$$(R_{\tau,t}^n)_m = \begin{cases} \max_{n' \in \mathcal{N}_n \cup \{n\}} (R_{\tau,t-1}^{n'})_m, & t > \tau \\ \mathbb{1}\{S_t^n \in \mathcal{S}_m\}, & t = \tau, \end{cases} \quad (17)$$

where  $\mathcal{N}_n$  is the (stochastic, time-varying) neighborhood of agent  $n$  at time  $t$ , and  $\mathbb{1}\{S_t^n \in \mathcal{S}_m\}$  is the direct observation that the state of agent  $n$  is in  $\mathcal{S}_m$  at time  $t$ . During each rollout  $k$ , agent  $n$  keeps the series of estimates  $R_{\tau,t}^n$ ,  $\tau = kT_0, \dots, (k+1)T_0 - 1$ , updating them recursively via (17) at each time  $t = \tau, \dots, (k+1)T_0 - 1$ .

Using these *gossiped* reward estimates to update the multipliers, the distributed version of (16) becomes

$$\lambda_{k+1}^n = \left[ (1 - \alpha)\lambda_k^n + \frac{\eta}{T_0} \sum_{\tau=kT_0}^{(k+1)T_0-1} (c - R_{\tau,(k+1)T_0-1}^n) \right]_+ \quad (18)$$

where agent  $n$  waits as much as possible until the end of the rollout at time  $t = (k+1)T_0 - 1$  to substitute  $R_{\tau,(k+1)T_0-1}$  for  $r(S_{\tau})$  and thus have the best possible estimate.

Equations (17) and (18), together with the policy structure in (10), are the main tools for the distributed implementation

**Algorithm 2:** Distributed multi-agent policy execution

---

```

1: for  $k = 0, 1, \dots$  do
2:   Substitute  $\lambda_n^k$  in (13) pretrained with local gradients.
3:   Keep the local realizable policy  $\pi_{\theta^n}[\lambda_n^k]$  as in (19).
4:   for  $t = kT_0, \dots, (k+1)T_0 - 1$  do
5:     Act  $A_t^n \sim \pi_{\theta^n}[\lambda_n^k]$  and transition to  $S_{t+1}^n$ .
6:     Collect local rewards  $(R_{t,t}^n)_m = \mathbb{1}\{S_t^n \in \mathcal{S}_m\}$ .
7:     Network gossiping: Update  $R_{\tau,t}^n$  as in (17).
8:   end for
9:   Update the multipliers according to (18).
10: end for

```

---

of the dual update, allowing agents to run the fully distributed policy in Algorithm 2.

In executing Algorithm 2, agents use a *realizable* policy  $\pi_{\theta}[\lambda^1, \dots, \lambda^N]$  in the sense that it is parametric, trained with finite rollouts as in (13), and with local copies of the multipliers. Specifically, each agent  $n$  substitutes its local copy of the vector of multipliers  $\lambda^n$  for  $\lambda$  in (10) to obtain its local part of the realizable policy  $\pi_{\theta^n}(A_t^n | S_t^n, \lambda^n)$ . Accordingly, the realizable global policy corresponds to their product

$$\pi_{\theta}[\lambda^1, \dots, \lambda^N](A_t | S_t) := \prod_{n=1}^N \pi_{\theta^n}(A_t^n | S_t^n, \lambda^n). \quad (19)$$

By using the distributed policies in (19), the team achieves the following realizable value

$$V_R := V_{T_0}(\pi_{\theta}[\lambda_k^1 \dots \lambda^N]) = \mathbb{E}_{\pi_{\theta}} \left[ \frac{1}{T_0} \sum_{t=kT_0}^{(K+1)T_0-1} r(S_t) \right]. \quad (20)$$

Because agents cannot guarantee to reach exact consensus on the multipliers  $\lambda^n$  almost surely when communicating over the stochastic graph (4), their realizable policies  $\pi_{\theta^n}(\lambda^n)$  will differ from the one  $\pi_{\theta^n}(\lambda)$  trained for, which assumed global access to  $\lambda$ . To mitigate the effect of this mismatch, we need the following assumption.

**Assumption 2** (Lipschitz continuity of value functions). *The difference between the value functions  $V_P$  and  $V_R$  with global and distributed multipliers, as defined in (14) and (20), respectively, is bounded by the scaled difference their multipliers with scaling constant  $L > 0$ , i.e.,*

$$\begin{aligned} \|V_P - V_R\| &= \|V_{T_0}(\pi_{\theta}[\lambda, \dots, \lambda]) - V_{T_0}(\pi_{\theta}[\lambda^1, \dots, \lambda^N])\| \\ &\leq L \max_{n=1, \dots, N} \|\lambda - \lambda^n\|_{\infty}. \end{aligned} \quad (21)$$

This assumption requires the parametric policies in (13) to be Lipschitz with respect to the multipliers, which is the case, for instance, if we choose neural networks for the policy parameterization with bounded weights and Lipschitz activation functions such as ReLU.

To quantify such an error, we measure the probability that the true rewards reach all agents. Referring back to Figures 1 and 2, the event that at time  $t$  agent  $n$  knows whether there is an agent  $n'$  that satisfied  $S_{t'}^{n'} \in \mathcal{S}_m$  at a previous time  $\tau$  is given by  $(R_{\tau,T}^n)_m = (r(S_{\tau}))_m$ . The distribution of that event

follows a negative binomial distribution, as is stated in the following proposition.

**Proposition 2.** *Given the Bernoulli graph model (4), the probability that agent  $n$  knows the global reward  $r(S_{\tau})$  at time  $t \geq \tau$  is*

$$\mathbb{P}((R_{\tau,t}^n)_m = (r(S_{\tau}))_m) \leq \mathbb{P}(BN(d_G, p) \leq t - \tau),$$

where  $d_G$  is the diameter of the underlying graph  $G$ ,  $p$  is the probability that an edge of the graph is active, and  $BN(d_G, p)$  denotes the negative binomial distribution.

*Proof.* See Appendix B. □

Leveraging Proposition 2, the following result provides a bound for the multipliers' error.

**Proposition 3.** *Given the Bernoulli graph model (4), the error norm between multipliers  $\lambda_k$  and  $\lambda_k^n$  in (16) and (18), computed in terms of the rewards  $r(S_{\tau})$  and their estimators  $R_{\tau,t}^n$ , respectively is bounded by*

$$\mathbb{E}[\|\lambda_k^n - \lambda_k\|_{\infty}] \leq \frac{\eta d_G}{\alpha T_0 p}, \quad (22)$$

where  $d_G$  is the diameter of the underlying graph  $G$ , and  $p$  is the probability that an edge of the graph is active.

*Proof.* See Appendix C. □

According to (22), the error between the global and local multipliers is controlled by the step size  $\eta$ , the contraction parameter  $\alpha$ , and the rollout horizon  $T_0$ . The trade-off for choosing  $T_0$  entails keeping the truncation error  $\epsilon$  in Assumption 1 sufficiently small and reducing the multipliers' error while ensuring that the multipliers are updated sufficiently often in order to speed training and increase the agents' agility in the online phase. Reducing  $\eta$  also reduces the bound in (22) at the expense of a slower dual update and policy reaction.

**Remark 1.** *Proposition 3 also demonstrates the role of  $\alpha$ . Including the contraction factor  $(1 - \alpha)$  in the dual update is key to guarantee that the deviation of the distributed multipliers remains bounded. Indeed, as the recursive addition of rewards accumulates over successive rollouts, the reward errors need to be modulated by powers of  $(1 - \alpha)$  to ensure that their aggregate effect in (22) is subdued. A higher  $\alpha$  makes the dual update more contractive, resulting in a smaller error in (22). However, increasing  $\alpha$  has an adverse effect on the feasibility guarantees, as we will establish in the next section.*

## IV. FEASIBILITY ANALYSIS

In this section we present the main result of our work which is to guarantee that the trajectories generated by Algorithm 2 are almost surely feasible in the sense that the time-averaged rewards exceed thresholds  $c$ , within an error controlled by the parameter  $\alpha$ , with probability one.

## A. Main Result

Before stating the feasibility guarantees we require an additional assumption regarding the underlying MDP.

**Assumption 3.** (*No repelling forces*). *The underlying Markov decision process is such that, given  $m$ , there exists a policy structured as in (7) which satisfies  $(r(S_t))_m = 1$  for all  $t$ .*

This assumption implies that, if necessary, an agent can keep its state stationed in a particular region  $S_t^n \in \mathcal{S}_m$ . We added this assumption for simplicity to attain  $(V)_m = 1$  and make the constraint  $m$  feasible with a margin  $1 - (c)_m$ . Assumption 3 can be substituted by a more general version  $(V)_m \geq c > (c)_m$ , only affecting the parameter  $\delta$  in the following Theorem 1. This milder version would hold, for instance, if  $S_t^n \in \mathcal{S}_m$  is attainable a fraction of time  $c \leq 1$ .

We are now in conditions to state our main result.

**Theorem 1.** *Let Assumptions 1–3 hold, and consider the specifications  $\|c\|_\infty < 1$ , and  $\|c\|_1 \leq N - 1$ . If*

$$\delta := (1 - \|c\|_\infty) - M(\epsilon + \beta) > 0, \quad (23)$$

*the trajectories generated by Algorithm 2 over the stochastic communication network (4) are feasible within an error  $\sqrt{\alpha M}$  with probability one, i.e.*

$$\liminf_{T \rightarrow \infty} \frac{1}{T} \sum_{t=0}^{T-1} r(S_t) \geq c - \mathbf{1}\sqrt{\alpha M}, \text{ a.s.} \quad (24)$$

*with  $\mathbf{1}$  being the vector of all ones and*

$$\alpha \geq \frac{\eta d_G M L}{p T_0 \delta}. \quad (25)$$

*Proof.* See Section IV-B.  $\square$

Since the constraints (3) involve time averages of binary rewards, the thresholds in  $c$  must be no larger than one for a feasible policy to exist. Theorem 1 imposes a stricter requirement  $\|c\|_\infty < 1$ , leaving a margin for the realizable policies. Also  $\|c\|_1 \leq N - 1$  is imposed, ensuring that  $N - 1$  agents can satisfy all constraints with a margin for the transients when agents' states cycle around regions  $\mathcal{S}_m$ . Additionally, condition (23) imposes limits on the approximation error in training, with  $\beta$  and  $\epsilon$  being the quantities defined in Assumption 1.

The result in Theorem guarantees that we can attain almost sure feasibility of a surrogate problem (3) where we tighten the constraints by increasing the thresholds to leave a margin for the error  $\sqrt{\alpha M}$  in (24), and we run Algorithms 1 and 2 using these surrogate thresholds. The value of  $\alpha$  in (25) can be made arbitrarily small by designing a rich parameterization or neural network, a long time horizon  $T_0$ , and a small step size  $\eta$ . These parameters introduce a trade-off between reducing the error and slowing training.

The result in Theorem 1 is derived by unrolling the stochastic dual recursion in (18) to write the sum of the rewards in terms of the multipliers, which yields an expression for the feasibility error in terms of the stochastic average of the multipliers along a trajectory. Hence, the proof is completed by bounding this stochastic average by  $\eta\sqrt{M}/\alpha$ . To obtain this bound for the stochastic average, we utilize proof techniques

similar to those in stochastic gradient descent on the dual domain, for which it is key to show that the gradient of the dual forms an acute angle with the vector of multipliers, i.e.

$$\lambda^\top (V - c) \geq 0. \quad (26)$$

In this direction, Lemma 1 below indicates that if we use the ideal policy  $\pi^*[\lambda, \dots, \lambda]$  in (6), the condition (26) is satisfied even with a slack  $(1 - \|c\|_\infty)\|\lambda\|/\sqrt{M}$ , that will become handy when considering the realizable policy in (20) instead. The proof of Lemma 1 uses Assumption 3 to ensure that the underlying MDP does not prevent the agents from taking care of the most pressing constraints. The value  $V$  in (2) and (26) assumes that we could train with infinite horizon, without the limitations of parametrization, and with all agents having access to the same multipliers in (16). On the other end,  $V_R$  in (20) corresponds to the realizable policy in Algorithm 2, and is obtained by applying the distributed, finite horizon and parametric procedures behind equations (13) and (18). In particular, each agent utilizes its own copy of local multipliers in (18). In between  $V$  and  $V_R$ , we defined  $V_P$  in (14) as a theoretical value to be used as an intermediate step in the proofs of feasibility. It differs from  $V$  in using a parametric policy and in aggregating the rewards for a finite time period of length  $T_0$ . And  $V_P$  is different from  $V_R$  in assuming global access by all agents to the same multipliers. We use Assumptions 1 and 2 in Lemma 2 to bound the difference  $\lambda^\top (V - V_R)$ . If this difference is lower than the slack  $(1 - \|c\|_\infty)\|\lambda\|/\sqrt{M}$ , then (26) will still be satisfied if we substitute  $V_R$  for  $V$ .

## B. Proof of Theorem 1 and Supporting Results

We proceed to prove our first result. The intuition in Lemma 1 is that if we fix  $\lambda$ , the ideal optimal policy assigns the  $N$  agents to the regions  $\mathcal{S}_m$  with highest weighted rewards. As the multipliers cycle in the execution phase according to Algorithm 2, this ideal behavior will drive the agents to cyclically attend the most pressing constraints at each rollout.

**Lemma 1.** *Assumption 3 with  $\|c\|_\infty < 1$  and  $\|c\|_1 \leq N - 1$  as in Theorem 1 results in*

$$\lambda^\top (V - c) \geq (1 - \|c\|_\infty) \frac{\|\lambda\|}{\sqrt{M}}. \quad (27)$$

*Proof.* Without loss of generality, sort the multipliers  $(\lambda)_1 \geq (\lambda)_2 \geq \dots \geq (\lambda)_M$ , so that  $(\lambda)_1$  is the largest multiplier.

One policy that optimizes the Lagrangian would assign an agent to each region  $\mathcal{S}_m$  of the state space for  $m = 1 \dots, N$ , since there are only  $N < M$  agents. Therefore,  $(V)_m = 1$  for  $m \leq N$  and  $(V)_m = 0$  for  $m > N$ . Hence it follows that

$$\lambda^\top (V - c) = (\lambda)_1 (1 - (c)_1) \quad (28)$$

$$+ \sum_{m=2}^N (\lambda)_m (1 - (c)_m) + \sum_{m=N+1}^M (\lambda)_m (0 - (c)_m).$$

Next, we use the fact that  $(c)_1 \leq \|c\|_\infty$  by definition of the infinity norm, so that  $(1 - (c)_1) \leq (1 - \|c\|_\infty)$ . Also, the multipliers were sorted in decreasing order which implies that the first one is maximum  $(\lambda)_1 = \|\lambda\|_\infty$ , the following  $N - 1$

satisfy  $(\lambda)_m \geq (\lambda)_N$  for all  $2 \leq m \leq N$ , and the last  $M - N$  satisfy  $(\lambda)_m \leq (\lambda)_N$  for all  $m > N$ . Hence, we bound the three terms in (28) by

$$\begin{aligned} \lambda^\top (V - c) &\geq (1 - \|c\|_\infty) \|\lambda\|_\infty \\ &+ (\lambda)_N \sum_{m=2}^N (1 - (c)_m) - (\lambda)_N \sum_{m=N+1}^M (c)_m \\ &\geq (1 - \|c\|_\infty) \|\lambda\|_\infty + (\lambda)_N ((N-1) - \|c\|_1), \end{aligned} \quad (29)$$

where we grouped the terms multiplying  $\lambda_N$  and then used  $\|c\|_1 = \sum_{m=1}^M (c)_m \geq \sum_{m=2}^M (c)_m$ . Given that  $(N-1) \geq \|c\|_1$  by hypothesis, we can write

$$\lambda^\top (V - c) \geq (1 - \|c\|_\infty) \|\lambda\|_\infty. \quad (30)$$

Then use the property  $\|\lambda\|_\infty \geq \|\lambda\|/\sqrt{M}$ .  $\square$

The following results bounds the error incurred in executing the realizable policy (19) as compared to the ideal policy (7). Intuitively, Lemma 2 guarantees that when agents use the realizable policy, they still behave as in the ideal case of Lemma 1, attending the most pressing constraints during the current rollout. Its proof uses Assumption 1 to bound the error between  $V$  and  $V_P$ , and Assumption 2 together with Proposition 3 for the error between  $V_P$  and  $V_R$ .

**Lemma 2.** *Given the stochastic communication network model (4), Assumptions 1–2 ensure that the following bound holds for the difference between the gradient of the ideal and realizable value functions*

$$(\lambda_k)^\top (V - V_R) \leq \|\lambda_k\| \left( \epsilon + \beta + \eta L \sqrt{M} \frac{d_G}{\alpha T_0 p} \right), \quad (31)$$

where  $V$  and  $V_R$  are defined in (2) and (20).

*Proof.* Write the norm of the difference between the ideal and realizable value functions as  $\|V_R - V\| \leq \|V - V_P\| + \|V_P - V_R\|$ , using the triangle inequality and summing and subtracting the term  $V_P$ . Hence, by Assumptions 1 and 2

$$\|V_R - V\| \leq \epsilon + \beta + L \max_{n=1, \dots, N} \|\lambda_k^n - \lambda_k\|_\infty, \quad (32)$$

and lastly, using Proposition 3, we obtain

$$\|V_R - V\| \leq \epsilon + \beta + L \epsilon_G = \epsilon + \beta + \eta L \sqrt{M} d_G / (\alpha T_0 p). \quad \square$$

Combining Lemmas 1 and 2, if conditions (23) and (25) in Theorem 1 are satisfied, then (26) holds for the realizable policy and  $V_R$ . Indeed, from (27) and (31) it yields

$$\begin{aligned} \lambda^\top (V_R - c) &= \lambda^\top (V - c) + \lambda^\top (V_R - V) \\ &\geq \frac{\|\lambda\|}{\sqrt{M}} \left( (1 - \|c\|_\infty) - M \left( \beta + \epsilon + \eta L \frac{d_G}{\alpha T_0 p} \right) \right) \geq 0, \end{aligned} \quad (33)$$

where the last inequality requires  $\delta > 0$  in (23) and it is equivalent to  $\alpha \geq \eta d_G M L / (p T_0 \delta)$  in (25).

Having a positive inner product in (33), we can prove that the stochastic average of the multipliers across a trajectory is bounded. This key result is presented below as Proposition 4. Its proof, relies on three steps. First, we combine (33) with the update (16) to obtain a contractive system with constant input for the expected value of  $\|\lambda\|$  conditioned on past values. From this contraction, it follows that the expected value of the

time average of the multipliers is bounded. Lastly, we include a modified proof of the strong law of large numbers for non-i.i.d. variables, which lets us drop the expected value and reach the following result.

**Proposition 4.** *Given the stochastic communication network model (4), under Assumptions 1–3, and with  $\|c\|_\infty < 1$ ,  $\|c\|_1 \leq N - 1$ ,  $\delta = (1 - \|c\|_\infty) - \sqrt{M}(\epsilon + \beta) > 0$ , and  $\alpha \geq \frac{\eta d_G}{p T_0} \cdot \frac{\sqrt{M} L}{\delta}$ , the averaged rewards along a trajectory are bounded by  $\eta \sqrt{M/\alpha}$  with probability 1, i.e.,*

$$\limsup_{k \rightarrow \infty} \frac{1}{k} \sum_{i=1}^k (\lambda_i)_m \leq \eta \sqrt{\frac{M}{\alpha}} \text{ a.s.} \quad (34)$$

*Proof.* See Appendix D.  $\square$

Hence, we proceed with the proof of Theorem 1. It yields from applying the results of Proposition 4 to the update rule (16). Specifically, we introduce

$$\bar{r}_k^{T_0} = \frac{1}{T_0} \sum_{\tau=(k-1)T_0}^{kT_0-1} r(S_\tau), \quad (35)$$

which reduces notation and lets us rewrite the update (16) as

$$\begin{aligned} \lambda_{k+1} &= \left[ (1 - \alpha) \lambda_k + \eta \left( c - \bar{r}_k^{T_0} \right) \right]_+ \\ &\geq (1 - \alpha) \lambda_k + \eta \left( c - \bar{r}_k^{T_0} \right), \end{aligned} \quad (36)$$

where the inequality that arises from the projection must be understood component-wise. Thus, from (36), we can rewrite

$$\eta \left( \bar{r}_k^{T_0} - c \right) \geq (1 - \alpha) \lambda_k - \lambda_{k+1}. \quad (37)$$

Hence, assuming  $\lambda_0 = 0$ , adding over  $k = 0, \dots, K$

$$\begin{aligned} \sum_{k=0}^K \eta \left( \bar{r}_k^{T_0} - c \right) &\geq \sum_{k=0}^K (1 - \alpha) \lambda_k - \sum_{k=0}^K \lambda_{k+1} \\ &= \sum_{k=1}^K (1 - \alpha) \lambda_k - \sum_{k=1}^K \lambda_k - \lambda_{K+1} = - \sum_{k=1}^K \alpha \lambda_k - \lambda_{K+1}, \end{aligned} \quad (38)$$

where we removed the term corresponding to  $\lambda_0$ , substituted  $k = k + 1$  in the sum of  $\lambda_{k+1}$  and then rearranged two sums into one removing those terms  $\lambda_k$  that cancel each other. Moving  $c$  and  $\eta$  to the right-hand side, we further obtain

$$\frac{1}{K} \sum_{k=0}^K \bar{r}_k^{T_0} \geq c - \frac{1}{\eta K} \lambda_{K+1} - \frac{\alpha}{\eta} \frac{1}{K} \sum_{k=1}^K \lambda_k, \quad (39)$$

and using Proposition 4, results in

$$\liminf_{K \rightarrow \infty} \frac{1}{K} \sum_{k=1}^K \bar{r}_k^{T_0} \geq c - \alpha \sqrt{\frac{M}{\alpha}}. \quad (40)$$

We demonstrated throughout this section that selecting  $\alpha > 0$ , which is required according to Proposition 3 to ensure that the multiplier error remains bounded, introduces an error in the feasibility result (24). Thus, we want to make  $\alpha$  as small as possible, but this is limited by (25), which is imposed to ensure the dual descends according to (33). We can adjust  $\eta$  and  $T_0$  and  $p$  to reduce the lower bound for  $\alpha$  in (25). In particular, the activation probability  $p$  in the stochastic



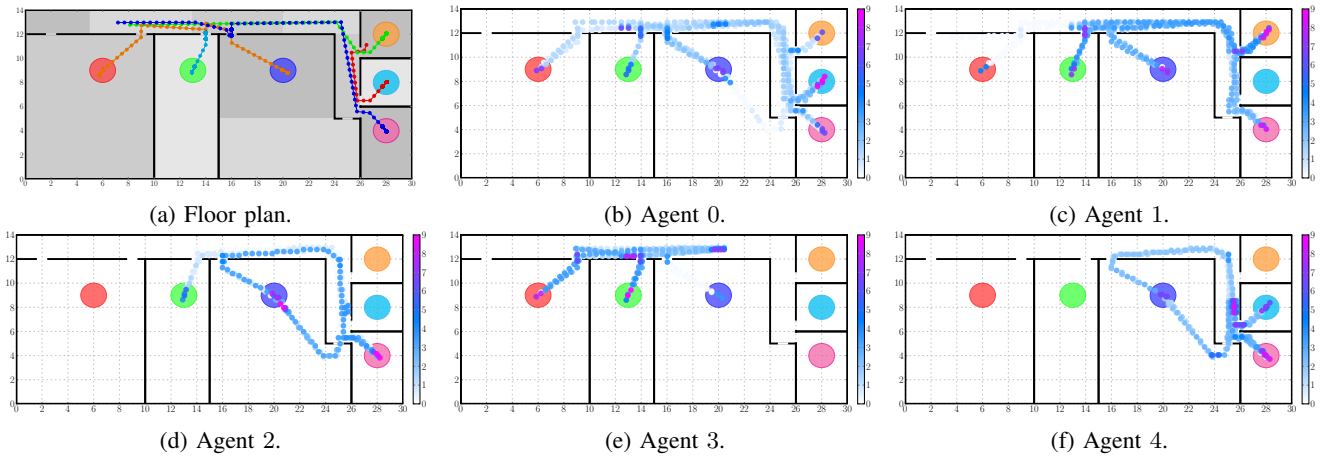


**Fig. 3:** (a) Floor plan and sample trajectories for each of the  $N = 5$  agents,  $n = 0, \dots, 4$ . Black lines represent walls, and colored circles represent the  $M = 6$  zones to be patrolled by the agents. Each colored dot along a trajectory indicates a new position for each time step. The 12 gray rectangular regions define distinct possible tiles or observations of an agent’s position, which are the inputs to the policy. Figures (b)–(f): Occupation heat maps. The complete trajectory of an agent across 40,000 timesteps is represented by dots, indicating the position reached by an agent. Each dot color represents the frequency of occupation at that position, with darker hues indicating more frequent positions, under a logarithmic colorbar scale.

communication graph depends on the communication scheme that is part of the problem design. In the next section, we provide an example of how to increase this probability by boosting the communication power.

## V. NUMERICAL EXPERIMENTS

In the following, we present numerical experiments designed to test the performance of the proposed multi-agent reinforcement learning Algorithm 2. We consider a scenario with five robots acting as agents, which navigate and monitor multiple rooms in a floor plan.

### A. Floor Plan Navigation

Consider  $N = 5$  agents navigating a floor plan of an L-shaped corridor connecting three offices and three laboratories at the University of Pittsburgh, with their separating walls represented as black lines (see Fig. 3). In this scenario, the state of agent  $n$  at time  $t$  is  $S_t^n = (x_t^n, y_t^n)$  with  $x_t^n$  and  $y_t^n$  representing the agent horizontal and vertical coordinates, respectively with  $S_t^n \in [0, 30] \times [0, 14]$ , all measured in meters. Correspondingly, the  $M = 6$  regions  $\mathcal{S}_1, \dots, \mathcal{S}_M$  are depicted by the colored circles in Fig. 3, centered at  $(x_1, y_1) = (6, 9)$ ,  $(x_2, y_2) = (13, 9)$ ,  $(x_2, y_2) = (20, 9)$ ,  $(x_3, y_3) = (28, 4)$ ,  $(x_4, y_4) = (28, 8)$ , and  $(x_5, y_5) = (28, 12)$ , and with all radius equal to one. The global reward corresponding to zone  $m$  takes the value  $(r(S_t))_m = 1$  if at least one agent enters the corresponding circle. The action space  $\mathcal{A} = \{0, \dots, 5\}$  is finite, meaning that the agents must decide which of the six regions to visit at each instant. We assume a low-level robot navigation control is available to drive the agent across the floor plan toward the selected zone. This controller follows a sequence of segments between intermediate goals located at a set of strategic points in rooms, corridors, and doors connecting any two rooms in the floor plan of Fig. 3.

Next, we describe in more detail how agents gain this ability to identify which zones they should visit by applying

Algorithms 1 and 2. First, each agent learns a set of optimal policy parameters offline using Algorithm 1. Specifically, each agent adopts a soft-max policy with exponents given by the  $M = 6$  logits in the output layer of a two-layer neural network with 256 hidden neurons whose inputs are the vector  $\lambda$  of  $M = 6$  multipliers and the coordinate  $S_t^n$  of the agent.

To optimize (13) for all agents efficiently, we take a block maximization approach in which individual agents retrain sequentially. We start this procedure by training a single agent in the floor plan environment to obtain a set of parameters  $\bar{\theta}$ . Then, all  $N$  agents’ policies are initialized with the same common parameter  $\theta^n = \bar{\theta}$ ,  $n = 1, \dots, N$ , and the retraining sequence starts. In each step of this sequence, an agent is selected to be the active learner, which updates its policy by running the iteration in Algorithm 1. All other agents follow trajectories driven by their policies, which remain unchanged. After the active agent retrains in these conditions, its policy settles, and the active token is passed on to the next agent.

During the online execution phase, all agents initialize their multipliers to zero and then update them following (18) with  $\alpha = 0.01$  and  $\eta = 0.5$ . For a span of  $T_0 = 100$  time steps, each agent will use the realizable policy described in Algorithm 2. They substitute their local copies  $\lambda_k^n \in \mathbb{R}^M$  of the vector of multipliers in the trained policy  $\pi_\theta(S_t, \lambda_k^n) = (\pi_{\theta^1}(S_t^1, \lambda_k^n), \dots, \pi_{\theta^N}(S_t^N, \lambda_k^n))$ , and then keep the  $n$ -th component  $\pi_{\theta^n}(S_t^n, \lambda_k^n)$ . Using this procedure, the agents do not need to know or exchange their local positions. Instead, the coordination is achieved through the dual multipliers (18), which are kept consistent among agents thanks to the network gossiping of reward estimations (17). As detailed in Section V-B below, the agents in this experiment gossip through an ad-hoc communication network that resembles the probabilistic model (4), in which two agents communicate if they are inline of sight or near each other.

The coordinated behavior in which the agents take complementary paths is observed in Fig. 3, where we show  $N = 5$

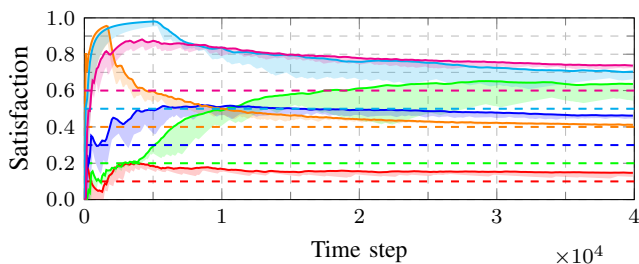


Fig. 4: Satisfaction of the constraints for each zone  $m = 1, \dots, 6$ . Constraint requirements were defined as 0.1 for zone 1, 0.2 for zone 2, etc. Dashed lines indicate these constraints. Minimum and maximum satisfaction values are plotted for each timestep for each zone and are filled by a shaded region. Colors of constraint and satisfaction values match those of the zones as depicted in Fig. 3.

heat maps, each corresponding to the trajectories of an agent during the online execution phase. Specifically, each of the  $N = 5$  color graphs in Fig. 3, one per agent, is obtained by dividing the floor plan into  $120 \times 56$  square bins of side  $dx = dy = 0.25$  and computing a two-dimensional histogram by counting how many times the agent enters each bin during a trajectory of  $T = 40,000$  time steps. The color scale is logarithmic, which implies that the agents occupy most of their time inside the circular regions. The paths in Fig. 3 demonstrate how the agents learn to coordinate in order to attend different regions and thus satisfy the competing constraints. The constraints for this numerical experiment are defined by the thresholds  $c = (0.1, 0.2, 0.3, 0.4, 0.5, 0.6)$  for the red, green, blue, orange, cyan, and magenta regions, respectively. Since the sum of these thresholds is  $\|c\|_1 = 2.1$  greater than one, a single agent working alone cannot satisfy the constraints. And because there are more zones  $M = 6$  than agents  $N = 5$  the constraints cannot be satisfied by placing an agent in each zone. By applying Algorithms 1 and 2, the agents learn to automatically achieve a high-level coordination in which agents  $n = 0, 1, 2, 3$  and 4 are sent to attend most of their time at the cyan, orange, blue, green and magenta zones, respectively, and they use their spare time to collaborate in satisfying the constraint corresponding to the red zone. The assignment is not trivial because it depends on the relative weights of the thresholds and the proximity of the zones. For instance, agent  $n = 3$  contributes most of its time to attending the red zone, but it is otherwise attending the green zone in the next room, so it is the closest one to help. Moreover, it is intuitive that the red and green zones can split an agent because they are associated with less demanding constraints.

Overall, the underlying mechanism agents use to coordinate is to let themselves be driven by the highest multipliers' values while avoiding flocking. The high-level control that drives the agents is akin to a standard dual-optimal dynamic, in which each multiplier (increases) decreases when its corresponding zone is (not) being attended, making it (more) less urgent for the agents to visit it. Indeed, the policies are trained to seek the highest weighted reward,  $r_\lambda(S_t) = \lambda^\top (r(S_t) - c) = \sum_{m=0}^M (\lambda)_m ((r(S_t) - c)_m)$  and this is achieved by setting to one the rewards  $(r(S_t))_m$  corresponding to the highest multipliers, as it was argued for the ideal policy  $\pi_I$  in the

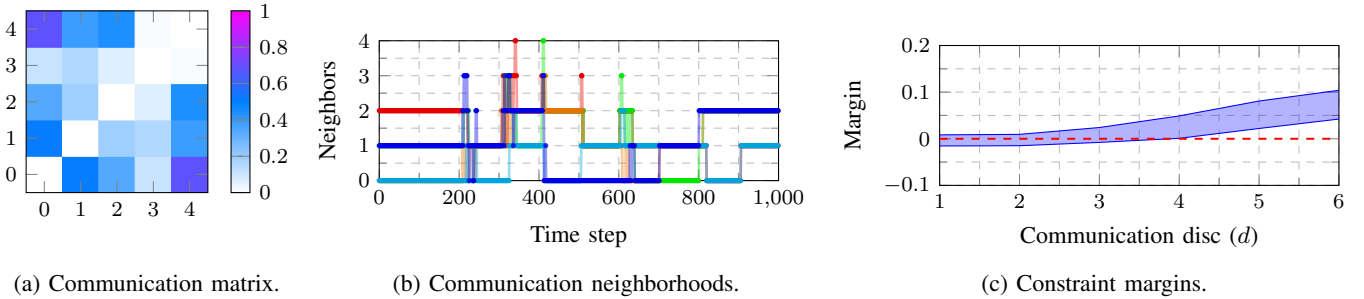
proof of Lemma 1.

Figure 4 presents the resulting performance in terms of constraint satisfaction. The dashed horizontal lines in Fig. 4 represent the thresholds  $c$  the agents must comply with. The colors correspond to the zones in Figure 3. The curves correspond to the long-run time averages  $\bar{r}(S_t) = \frac{1}{t} \sum_{\tau=0}^{t-1} r(S_\tau)$  over the span of 40,000 time steps. Notice that we use the global rewards  $r(S_t)$  as compared to  $R_{\tau,t}^n$ , even though they are never computed by the agents when running Algorithms 1 and 2, because these are the ones defining our original optimization problem (3). Accounting for the randomness of the reward trajectories, we run Algorithm 2 five times and report a band between the maximum and minimum values of the averaged rewards  $\bar{r}(S_t)$ . The results demonstrate that the agents can meet the specified constraints consistently for all runs so that all zones are adequately monitored over time, outperforming numerically the almost sure theoretical guarantees provided by Theorem 1.

### B. Communication over a Stochastic Graph

Purposely, the communication setup in the experiment described above does not exactly match the stochastic graph model with Bernoulli edges in (4). Instead, we consider a practical ad-hoc network that changes its connectivity as agents move across the floor plan. Specifically, two agents communicate if they are in the line of sight of each other regardless of their distance, or if they are closer than a range disc size  $d = 5$  meters separated by a wall. The fraction of time that each pair of agents communicate to each other along a trajectory of 40,000 steps is depicted in Fig. 5a. This representation shows that agents  $n = 0$  and  $n = 4$  remain connected most of the time, reflecting that they are within communication range, because they share similar paths and spend most of their time stationed in rooms next to each other. All agents connect to at least one other agent over time, enabling the gossip protocol (17) to succeed in passing the reward estimates between any two agents via multi-hop communications. Hence, the underlying static graph is connected, but not its stochastic samples, since the agent  $n = 3$  is frequently isolated from all other agents, probably when visiting the remote red zone, so that we would see a clustered network most of the time if we sampled the edges per time step. This intermittent communication connectivity plays a central role in the agents' behavior. For instance, Fig. 3a shows the blue trajectory of an agent entering the third room from the left but changing its path towards the magenta zone once it forms a line of sight with the orange agent attending the blue zone.

Another perspective of the network connectivity is given by the trajectories in Fig. 5b, which shows how the sizes of the communication neighborhoods evolve across time during a span of one thousand timesteps. There are five lines in Fig. 5b, representing the number of neighbors for each agent, with the same color-to-agent correspondence as in Fig. 3a. These trajectories corroborate that the agents do not flock together since they isolate reaching zero neighbors part of the time and are rarely connected to two other agents. It also shows that



**Fig. 5:** (a) Matrix of communication frequencies between agents, counted over time. For each pair of agents  $(n, n')$ , the number of timesteps during which these agents communicate is summed and divided by the total timesteps of simulation, 40,000. Frequencies are indicated by colors matching those in the included colorbar, with white indicating no communication. We define an agent as never communicating with itself, so diagonal entries are white. Figure (b): A snapshot of gossip neighborhood sizes per agent. Neighborhood sizes are plotted for 1,000 time-steps of execution phase.  $N = 5$  lines are present, one for each agent and of a color matching said agent’s trajectory in Fig 3. Figure (c): Margin of constraint satisfaction for each communication disc of sizes  $d = 1, \dots, 6$ . A minimum and maximum difference between satisfaction and constraint values across all zones  $m = 1, \dots, 6$  are found and plotted for each disc size, as indicated by the bold blue lines. A band shades the area between the maximum and minimum differences.

they seldom confer altogether, only two times in a thousand, so they need to transmit the rewards across the stochastic network by moving and passing messages dynamically. We can also infer from Fig. 5b that the agents cannot remain static in a zone during the total span of the experiment. The communication neighborhoods change dynamically as agents adjust their trajectories and spend part of their time for communication purposes, alternating between zones aiming to increase their joint reward and exchange information with their pairs. This behavior aligns with the observation that none of the agents hold their position throughout the experiment in Fig. 3, which is reasonable from the algorithmic perspective since an isolated agent sitting in a zone would see all other  $M - 1$  multipliers growing, and it would be therefore inclined to move to attend their corresponding zones, leaving its own.

Finally, we analyze how varying the communication range affects performance. Fig. 5c examines the margin of constraint satisfaction relative to the size of the communication disc  $d$ . For  $d = 1, \dots, 6$ , the blue lines represent the minimum difference between the average rewards and constraint thresholds across zones at time  $t = 40,000$ . That is,  $\min_m(\bar{r}_{40,000} - c)_m$ . The experiment is repeated five times to account for the randomness in the trajectories, and a band between the maximum and the minimum margin is presented in Fig. 5c.

The results show that the margin of constraint satisfaction results in negative values for small values of  $d$ , therefore not complying with primal problem (3), increasing above 0 for when the communication range increases above  $d = 4$ . This dependence of the margin with  $d$  aligns with our theory in Theorem 1, considering that a larger disc corresponds with a higher probability  $p$ . Thus, (24) tells us that the error of feasibility becomes smaller when  $\alpha$  decreases, which according to (25) is driven by increasing the probability  $p$ . Alternatively, for a fixed value of the parameter  $\alpha$ , equation (25) can only be satisfied if  $p$  becomes big enough.

In summary, these numerical experiments illustrated how our coordinated offline training, dual dynamics, and gossiping protocol provide a system of multiple agents with the ability to coordinate their actions. The simplified stochastic graph

model for communication in (4) has the virtue of being tractable, which allowed us to advance our analysis of feasibility summarized in Theorem 1 while capturing the necessary properties of a more realistic distance-defined network in terms of probabilities and time-evolving connectivity. Hence, the experiments abide by the theory, so the numerical results corroborate our theoretical feasibility guarantees.

## VI. CONCLUSION

In this work, we demonstrated the effectiveness of CMARL in complex coordination problems in which agents must solve competing tasks. By employing a state augmentation framework with non-convergent dual variables, we enabled agents to dynamically adapt their policies based on real-time constraint satisfaction levels. The integration of a gossiping protocol allowed agents to share local reward estimations across a stochastic network with one-bit communication, eliminating the need for direct state access and ensuring robust coordination. Our proposed contractive update rule for dual variables further enhanced scalability and feasibility without relying on exponentially growing memory buffers. We established theoretical guarantees of almost sure feasibility, as formalized in our main theorem, and validated our approach through numerical experiments. In these experiments, a team of robots successfully patrolled multiple regions under realistic communication constraints and intermittent connectivity, showcasing the practical applicability of our framework.

## APPENDIX

### A. Proof of Proposition 1

*Proof.* (Proposition 1) The separable structure of our training policy  $\pi_\theta(A_t | S_t, \lambda, \dots, \lambda) = \prod_{n=1}^N \pi_{\theta_n}(A_{tn} | S_{tn}, \lambda)$  yields  $\nabla_{\theta_n} \log \pi_\theta(S_t, A_t) = \nabla_{\theta_n} \log \pi_{\theta_n}(A_{tn} | S_{tn})$ .

Substituting the right-hand side in the policy gradient [41], we obtain  $\nabla_{\theta_n} \mathcal{L}(\pi_\theta, \lambda) = \mathbb{E}[L_n Q_{\pi_\theta}(S_t, A_t, \lambda)]$ , with  $L_n = \nabla_{\theta_n} \log \pi_{\theta_n}(A_{tn} | S_{tn})$ . Thus, using the law of total expectation, conditioning on  $S_{tn}, A_{tn}$ , we obtain

$$\nabla_{\theta_n} \mathcal{L}(\pi_\theta, \lambda) = \mathbb{E}_{(S_t^p, A_t^p)} \left[ \mathbb{E}_{(S_t, A_t)} [L_n Q_{\pi_\theta}(S_t, A_t, \lambda) | S_t^n, A_t^n] \right]$$

$$= \mathbb{E}_{S_t^n, A_t^n} \left[ L_n \mathbb{E}_{(S_t, A_t)} [Q_{\pi_\theta}(S_t, A_t, \lambda) \mid S_t^n, A_t^n] \right], \quad (41)$$

to then substitute  $Q_{\pi_\theta}^n(\cdot)$  as defined in (12) into (41).  $\square$

### B. Proof of Proposition 2

*Proof.* (Proposition 2) Consider two agents  $J < d_G$  nodes apart. For a particular journey of times waiting to cross each intermediate edge  $(t_1, t_2, \dots, t_J)$ , the probability is

$$p(t_1, t_2, \dots, t_J) = p \cdot (1-p)^{t_1-1} \cdot p \cdot (1-p)^{t_2-1} p \dots (1-p)^{t_J-1},$$

where  $p$  is the stochastic graph's communication probability. To compute the probability of  $r(S_\tau)$  reaching agent  $n$  at time  $t = \tau + i$ , exactly  $i$  steps after  $\tau$ , observe that there are as many combinations of  $(t_1, t_2, \dots, t_J)$  as  $\binom{i-1}{J-1}$ , i.e. ways of having  $J-1$  successes over  $i-1$  time steps. This count corresponds to a negative binomial variable  $BN_{p,J}(i)$ .

Consequently, the reward associated with the  $m$ -th constraint at time  $\tau$ , that is  $(r(S_\tau))_m$ , will reach agent  $n$  on time at time  $(k+1)T_0 - 1$  or before with probability

$$\mathbb{P}((e_\tau)_m = 0) = \mathbb{P}\left(\left(r(S_\tau) = R_{\tau, (k+1)T_0-1}^n\right)_m\right) \quad (42)$$

$$\leq \mathbb{P}(BN(J, p) \leq (k+1)T_0 - 1 - \tau) \quad (43)$$

$$\leq \mathbb{P}(BN(d_G, p) \leq (k+1)T_0 - 1 - \tau), \quad (44)$$

where the first inequality appears because the error  $e_\tau = r(S_\tau) - R_{\tau, (k+1)T_0-1}^n$  is null if  $r(S_\tau) = 0$  even if the message fails to reach agent  $n$ , and the second one is because the probability of a negative binomial becomes lower when the number of required successes is increased. Correspondingly,

$$\mathbb{P}((e_\tau)_m = 1) \leq \mathbb{P}\left(BN(d_G, p) > (k+1)T_0 - 1 - \tau\right), \quad (45)$$

which concludes the proof.  $\square$

### C. Proof of Proposition 3

*Proof.* (Proposition 3) We can use the previous result to bound the expected error during a rollout. Since the entries of  $e_\tau$  in (42) can only take values zero or one, we can write

$$\mathbb{E} \left[ \sum_{t=kT_0}^{(k+1)T_0-1} \left( r(S_\tau) - R_{\tau, (k+1)T_0-1}^n \right)_m \right] \quad (46)$$

$$= \sum_{\tau=kT_0}^{(k+1)T_0-1} \mathbb{P}((e_\tau)_m = 1) \quad (47)$$

$$\leq \sum_{\tau=kT_0}^{(k+1)T_0-1} \mathbb{P}\left(BN(d_G, p) > (k+1)T_0 - 1 - \tau\right) \quad (48)$$

$$= \sum_{l=0}^{T_0} \mathbb{P}\left(BN(d_G, p) > l\right) \leq \sum_{l=0}^{\infty} \mathbb{P}\left(BN(d_G, p) > l\right) \quad (49)$$

$$= \mathbb{E}[BN(d_G, p)] = \frac{d_G}{p},$$

where we used (45), substituted  $l = (k+1)T_0 - 1 - \tau$ , and added the tail to the sum so that it equals the expectation in (49), which is  $d_G/p$  for the negative binomial. To associate this

expected value with the error between multipliers, we consider a particular agent  $n$ , take the difference between the global and local updates in (16) and (18), and bound the expectation as

$$\mathbb{E} \left[ \|\lambda_{k+1}^n - \lambda_{k+1}\|_\infty \right] \quad (50)$$

$$\leq \frac{\eta}{T_0} \mathbb{E} \left[ \left\| \sum_{\tau=kT_0}^{(k+1)T_0-1} \left( r(S_\tau) - R_{\tau, (k+1)T_0-1}^n \right) \right\|_\infty \right] \quad (51)$$

$$+ (1-\alpha) \mathbb{E} \left[ \|\lambda_k^n - \lambda_k\| \right] \leq \frac{\eta d_G}{T_0 p} + (1-\alpha) \mathbb{E} \left[ \|\lambda_k^n - \lambda_k\|_\infty \right].$$

Unrolling (50) with  $\lambda_0^n = \lambda_0$ , we obtain

$$\mathbb{E} \left[ \|\lambda_{k+1}^n - \lambda_{k+1}\| \right] \leq \sum_{i=0}^k (1-\alpha)^i \frac{\eta d_G}{T_0 p} \leq \frac{\eta d_G}{T_0 \alpha p},$$

which concludes the proof.  $\square$

### D. Proof of Proposition 4

The proof of Proposition 4 relies on the following four Lemmas, which show that the multipliers follow a contractive evolution in a martingale sense (Lemma 3), which allows us to prove both that their expected running averages are bounded by  $\mathcal{O}(1/\sqrt{\alpha})$  (Lemma 4), and that they are deterministically bounded by a larger constant (Lemma 1). This deterministic bound is a technicality to show that we can drop the expectation from Lemma 4) and bound the stochastic running averages by  $\mathcal{O}(1/\sqrt{\alpha})$  (Lemma 6) which is the claim of Proposition 4.

**Lemma 3.** *Given the stochastic communication network model (4), under Assumptions 1–3, and with  $\|c\|_\infty < 1$ ,  $\|c\|_1 \leq N-1$ ,  $\delta = (1 - \|c\|_\infty) - M(\beta + \varepsilon_{T_0}) > 0$  and  $\alpha \geq \frac{\eta d_G}{p T_0} \frac{M L}{\delta}$ , the multipliers satisfy the following inequality*

$$\mathbb{E} \left[ \|\lambda_k\|^2 \mid \mathcal{F}_{k-1} \right] \leq (1-\alpha)^2 \|\lambda_{k-1}\|^2 + \eta^2 M. \quad (52)$$

*Proof.* As in the proof of Theorem 1 we use  $\bar{r}_k^{T_0} = \frac{1}{T_0} \sum_{\tau=(k-1)T_0}^{kT_0-1} r(S_\tau)$  to denote the average reward during the  $k$ -th rollout, and rewrite the multiplier recursion (16) as

$$\lambda_{k+1} = \left[ (1-\alpha)\lambda_k + \eta \left( c - \bar{r}_k^{T_0} \right) \right]_+. \quad (53)$$

Then, we use that projections reduce distances to bound

$$\mathbb{E} \left[ \|\lambda_{k+1}\|^2 \mid \mathcal{F}_k \right] = \mathbb{E} \left[ \left\| \left[ (1-\alpha)\lambda_k + \eta \left( c - \bar{r}_k^{T_0} \right) \right]_+ \right\|^2 \mid \mathcal{F}_k \right]$$

$$\leq \mathbb{E} \left[ \left\| (1-\alpha)\lambda_k + \eta \left( c - \bar{r}_k^{T_0} \right) \right\|^2 \mid \mathcal{F}_k \right] \quad (54)$$

$$\leq (1-\alpha)^2 \|\lambda_k\|^2 + 2(1-\alpha)\eta \lambda_k^T \mathbb{E} \left[ c - \bar{r}_k^{T_0} \mid \mathcal{F}_k \right] \quad (55)$$

$$+ \eta^2 \mathbb{E} \left[ \left\| c - \bar{r}_k^{T_0} \right\|^2 \mid \mathcal{F}_k \right] \quad (56)$$

$$\leq (1-\alpha)^2 \|\lambda_k\|^2 + 2(1-\alpha)\eta \lambda_k^T \mathbb{E} \left[ c - \bar{r}_k^{T_0} \mid \mathcal{F}_k \right] + \eta^2 M,$$

where we bounded  $(c - \bar{r}_k^{T_0})_m^2 < 1$ .

The expectation above must be taken with respect to the realizable policy  $\pi_\theta[\lambda_k^1, \dots, \lambda_k^N]$  in (19), since we want to



obtain results for stochastic trajectories following that policy. Thus  $\mathbb{E}[\bar{r}_k^{T_0} | \mathcal{F}_k] = V_R$  as defined in (20), so that

$$\mathbb{E}[\|\lambda_{k+1}\|^2 | \mathcal{F}_k] \leq (1 - \alpha)^2 \|\lambda_k\|^2 \quad (57)$$

$$+ 2(1 - \alpha)\eta\lambda_k^T(c - V_R) + \eta^2 M, \quad (58)$$

and we showed in (33) that, under the hypotheses of Lemmas 1 and 2,  $\lambda_k^T(c - V_R) \leq 0$ , which let us conclude the proof by removing the second term in the right-hand side of (58).  $\square$

**Lemma 4.** *Under the hypothesis of Lemma 3*

$$\limsup_{k \rightarrow \infty} \frac{1}{k} \sum_{i=1}^k \mathbb{E}[(\lambda_i)_m] \leq \eta \sqrt{\frac{M}{\alpha}}. \quad (59)$$

*Proof.* Using (52) we obtain

$$\mathbb{E}[\|\lambda_k\|^2] \leq (1 - \alpha)^2 \mathbb{E}[\|\lambda_{k-1}\|^2] + \eta^2 M. \quad (60)$$

Thus, by induction starting from  $\lambda_0 = 0$  for convenience

$$\mathbb{E}[\|\lambda_k\|^2] \leq \sum_{j=0}^{k-1} (1 - \alpha)^{2j} \eta^2 M \leq \eta^2 M \sum_{j=0}^{\infty} (1 - \alpha)^{2j} \quad (61)$$

$$= \frac{\eta^2 M}{(1 - (1 - \alpha)^2)} \leq \frac{\eta^2 M}{\alpha}. \quad (62)$$

Applying Jensen's inequality and then (62), we can bound the moment of  $\lambda_{k+1}$  by  $(\mathbb{E}[\|\lambda_{k+1}\|])^2 \leq \mathbb{E}[\|\lambda_{k+1}\|^2] \leq \frac{\eta^2 M}{\alpha}$  which yields the following bound for the expected value of each entry of  $\lambda_k$ ,  $\mathbb{E}[(\lambda_k)_m] \leq \mathbb{E}[\|\lambda_k\|] \leq \eta \sqrt{\frac{M}{\alpha}}$ .  $\square$

In the next lemma, we prove that the multipliers are deterministically bounded by a constant  $U$  of order  $\mathcal{O}(1/\alpha)$ , deriving this result directly from the contractive form of the stochastic update (16). Thus, it is immediate that the stochastic time average (34) in Proposition 4 is bounded by  $U$  too. Although more complex, the argument in the proof of Proposition 4 is meaningful because it yields a tighter bound of order  $\mathcal{O}(1/\sqrt{\alpha})$  as in (34). Hence, the feasibility error (24) in Theorem 1, which results from multiplying the bound (34) by  $\alpha$  in (40), can be controlled by the design parameter  $\alpha$ .

**Lemma 5.** *Under the hypothesis of Lemma 3, the multipliers  $\lambda_k$  in (16) are bounded almost surely by  $U = \eta\sqrt{M}/\alpha$ .*

*Proof.* From the update 16 written as in 53, yields

$$\|\lambda_{k+1}\| \leq \left\| \lambda_k(1 - \alpha) + \eta \left( c - \bar{r}_k^{T_0} \right) \right\| \quad (63)$$

$$\leq (1 - \alpha) \|\lambda_k\| + \eta \left\| c - \bar{r}_k^{T_0} \right\| \leq (1 - \alpha) \|\lambda_k\| + \eta\sqrt{M}$$

$$\leq (1 - \alpha)^k \|\lambda_0\| + \sum_{j=0}^k \eta\sqrt{M}(1 - \alpha)^j \quad (64)$$

$$\leq \eta\sqrt{M} \sum_{j=0}^{\infty} (1 - \alpha)^j = \frac{\eta\sqrt{M}}{\alpha}, \quad (65)$$

where we assumed  $\lambda_0 = 0$  for convenience.  $\square$

**Lemma 6.** *Assume that there exists a constant  $C > 0$  such that  $\limsup_{k \rightarrow \infty} \frac{1}{k} \sum_{i=1}^k \mathbb{E}[(\lambda_i)_m] \leq C$ . Then the following bound also holds with probability one for the average stochastic multipliers, i.e.,  $\limsup_{k \rightarrow \infty} \frac{1}{k} \sum_{i=1}^k (\lambda_i)_m \leq C$ .*

*Proof.* Define  $\ell_{k+1} := \lambda_{k+1} - \mathbb{E}[\lambda_{k+1} | \mathcal{F}_k]$ . We start by proving that these  $\ell_k$  satisfy the SLLN. By definition, these variables are zero-mean conditioned on  $\mathcal{F}_k$ , and they are deterministically bounded by  $2U$  according to Lemma 5, but they are not i.i.d. because  $\lambda_k$  accumulates rewards. Then, to prove that  $\mu_k := \frac{1}{k+1} \sum_{i=0}^k \ell_i \xrightarrow{a.s.} 0$ , consider the partial sums  $U_{k+1} = \sum_{i=1}^{k+1} \ell_i = \ell_{k+1} + U_k$ . Since  $\ell_{k+1}$  are conditionally zero-mean,  $U_k$  is a martingale, i.e.,

$$\mathbb{E}[U_{k+1} | \mathcal{F}_k] = \mathbb{E}[\ell_{k+1} | \mathcal{F}_k] + U_k = U_k. \quad (66)$$

To use the proof of the SLLN in [44, p.456], we need a bound for the second moment of  $U_k$  that increases with order  $k$  at most. Without the standard i.i.d. assumption, we write

$$\mathbb{E}[\|U_{k+1}\|^2 | \mathcal{F}_k] = \|U_k\|^2 + 2U_k^T \mathbb{E}[\ell_{k+1} | \mathcal{F}_k] \quad (67)$$

$$+ \mathbb{E}[\|\ell_{k+1}\|^2 | \mathcal{F}_k] \leq \|U_k\|^2 + U^2. \quad (68)$$

Conditioning to  $\mathcal{F}_{k-1}$  instead, we bound

$$\mathbb{E}[\|U_{k+1}\|^2 | \mathcal{F}_{k-1}] = \mathbb{E}[\mathbb{E}[\|U_{k+1}\|^2 | \mathcal{F}_k] | \mathcal{F}_{k-1}] \quad (69)$$

$$\leq \mathbb{E}[\|U_k\|^2 + U^2 | \mathcal{F}_{k-1}] \leq \mathbb{E}[\|U_k\|^2 | \mathcal{F}_{k-1}] + U^2 \quad (70)$$

$$\leq \|U_{k-1}\|^2 + U^2 + U^2. \quad (71)$$

If we repeat this process recursively, reducing the time index of the filtration, we arrive at  $\mathbb{E}[\|U_{k+1}\|^2 | \mathcal{F}_0] = \mathbb{E}[\|U_{k+1}\|^2]$ , obtaining the following bound for the unconditional moment of  $U_{k+1}$

$$\mathbb{E}\|U_{k+1}\|^2 \leq \mathbb{E}\|U_1\|^2 + kU^2 = \mathbb{E}\|\lambda_0\|^2 + (k+1)U^2 \quad (72)$$

$$\leq U^2 + kU^2 \leq (k+1)U^2. \quad (73)$$

Henceforth, we can substitute  $X_i$  and  $S_n$  for  $\ell_i$  and  $U_k$ , respectively, and follow the proof in [44, p.456] to conclude

$$\mu_k := \frac{1}{k+1} \sum_{i=0}^k \ell_i = \frac{1}{k+1} \sum_{i=0}^k (\lambda_i - \mathbb{E}[\lambda_i | \mathcal{F}_{i-1}]) \xrightarrow{a.s.} 0.$$

Next, we want to get rid of the filtrations and compare the stochastic running average to the average of unconditional expectations. Specifically, we want  $\frac{1}{k} \sum_{i=1}^k (\lambda_i - \mathbb{E}[\lambda_i]) \xrightarrow{a.s.} 0$ . To that end, consider  $\bar{\lambda}_{k+1}^{(k)} = \mathbb{E}[\lambda_{k+1} | \mathcal{F}_k] = \mathbb{E}[\lambda_{k+1} | \lambda_k]$ , which is a random variable that is a function of  $\lambda_k$  for  $k > 1$ , and with the convention  $\mathbb{E}[\lambda_k | \mathcal{F}_{k-1}] = \mathbb{E}[\lambda_i]$  if  $k \leq 1$ . Thus, we can use a recursive argument by redefining the conditionally zero-mean

$$\ell_{k+1} = \bar{\lambda}_{k+1}^{(k)} - \mathbb{E}[\bar{\lambda}_{k+1}^{(k)} | \mathcal{F}_{k-1}] = \mathbb{E}[\lambda_{k+1} | \mathcal{F}_k] - \mathbb{E}[\lambda_{k+1} | \mathcal{F}_{k-1}],$$

which are also bounded by  $U$ , hence we can apply the SLLN again to the corresponding time averages

$$\mu_k = \frac{1}{k} \sum_{i=1}^k \ell_i = \frac{1}{k} \sum_{i=1}^k (\mathbb{E}[\lambda_i | \mathcal{F}_{i-1}] - \mathbb{E}[\lambda_i | \mathcal{F}_{i-2}]) \xrightarrow[k \rightarrow \infty]{a.s.} 0.$$

Then we can move backwards on time by repeating this argument for previous  $i - n + 1$  and  $i - n$ , i.e.,

$$\mu_k = \frac{1}{k} \sum_{i=1}^k (\mathbb{E}[\lambda_i | \mathcal{F}_{i-n+1}] - \mathbb{E}[\lambda_i | \mathcal{F}_{i-n}]) \xrightarrow[k \rightarrow \infty]{a.s.} 0,$$

and the conditioning can be removed when we reach  $n \geq k$ , resulting in  $\mathbb{E}[\lambda_i | \mathcal{F}_{i-k}] = \mathbb{E}[\lambda_i]$ , for all  $i \leq k$ , which implies that the stochastic and expected running averages coincide. Hence, our result follows.  $\square$

Finally, put the lemmas together to prove the proposition.

*Proof.* (Proposition 4)

Substitute  $C = \eta \sqrt{\frac{M}{\alpha}}$  from Lemma 4 in Lemma 6.  $\square$

## REFERENCES

- [1] L. Canese et al. “Multi-agent reinforcement learning: A review of challenges and applications”. In: *Applied Sciences* 11.11 (2021), p. 4948.
- [2] K. Zhang, Z. Yang, and T. Başar. “Multi-agent reinforcement learning: A selective overview of theories and algorithms”. In: *Handbook of reinforcement learning and control* (2021), pp. 321–384.
- [3] Y. Yang et al. “Believe what you see: Implicit constraint approach for offline multi-agent reinforcement learning”. In: *Advances in Neural Information Processing Systems* 34 (2021), pp. 10299–10312.
- [4] L. Busoniu, R. Babuska, and B. De Schutter. “A comprehensive survey of multiagent reinforcement learning”. In: *IEEE Trans. on Sys., Man, and Cyber., Part C (App. and Reviews)* 38.2 (2008), pp. 156–172.
- [5] Y. Lin et al. “Multi-agent reinforcement learning in stochastic networked systems”. In: *Adv. in neural information proc. systems* 34 (2021), pp. 7825–7837.
- [6] N. Bard et al. “The hanabi challenge: A new frontier for ai research”. In: *Artificial Intel.* 280 (2020), p. 103216.
- [7] B. Baker et al. “Emergent tool use from multi-agent autocurricula”. In: *preprint arXiv:1909.07528* (2019).
- [8] H. Wei et al. “Colight: Learning network-level cooperation for traffic signal control”. In: *Proceedings of the 28th ACM international conference on information and knowledge management.* 2019, pp. 1913–1922.
- [9] G. Kahn et al. “Uncertainty-aware reinforcement learning for collision avoidance”. In: *arXiv preprint arXiv:1702.01182* (2017).
- [10] D. Isele, A. Nakhaei, and K. Fujimura. “Safe reinforcement learning on autonomous vehicles”. In: *2018 IEEE/RSJ International Conference on Intelligent Robots and Systems (IROS)*. IEEE. 2018, pp. 1–6.
- [11] T.-Y. Yang et al. “Safe reinforcement learning for legged locomotion”. In: *2022 IEEE/RSJ International Conference on Intelligent Robots and Systems (IROS)*. IEEE. 2022, pp. 2454–2461.
- [12] J. Hwangbo et al. “Learning agile and dynamic motor skills for legged robots”. In: *Science Robotics* 4.26 (2019), eaau5872.
- [13] J. Ibarz et al. “How to train your robot with deep reinforcement learning: lessons we have learned”. In: *Int. J. of Robotics Research* 40.4-5 (2021), pp. 698–721.
- [14] J. Kober, J. A. Bagnell, and J. Peters. “Reinforcement learning in robotics: A survey”. In: *Int. J. of Robotics Research* 32.11 (2013), pp. 1238–1274.
- [15] Y. Chen and A. D. Ames. “Probabilistic safety constraints for reinforcement learning”. In: *IEEE Transactions on Automatic Control* (2024).
- [16] W. Chen, D. Subramanian, and S. Paternain. “Probabilistic constraint for safety-critical reinforcement learning”. In: *IEEE Trans. on Automatic Control* (2024).
- [17] J. Garcia and F. Fernández. “A comprehensive survey on safe reinforcement learning”. In: *J. of Machine Learning Res.* 16.1 (2015), pp. 1437–1480.
- [18] Q. Liang, F. Que, and E. Modiano. “Accelerated primal-dual policy optimization for safe reinforcement learning”. In: *Advances in Neural Information Processing Systems* (2017).
- [19] A. Castellano et al. “Learning to act safely with limited exposure and almost sure certainty”. In: *IEEE Trans. on Aut. Control* 68.5 (2023), pp. 2979–2994.
- [20] J. Cui, Y. Liu, and A. Nallanathan. “Multi-Agent Reinforcement Learning-Based Resource Allocation for UAV Networks”. In: *IEEE Transactions on Wireless Communications* 19.2 (2020), pp. 729–743.
- [21] W. Qin et al. “Multi-agent reinforcement learning-based dynamic task assignment for vehicles in urban transportation system”. In: *International Journal of Production Economics* 240 (2021), p. 108251.
- [22] S. Gu et al. “Multi-agent constrained policy optimisation”. In: *preprint arXiv:2110.02793* (2021).
- [23] Y.-J. Chen, D.-K. Chang, and C. Zhang. “Autonomous tracking using a swarm of UAVs: A constrained multi-agent reinforcement learning approach”. In: *IEEE Transactions on Vehicular Technology* 69.11 (2020), pp. 13702–13717.
- [24] S. Liu and M. Zhu. “Distributed inverse constrained reinforcement learning for multi-agent systems”. In: *Advances in Neural Information Processing Systems* 35 (2022), pp. 33444–33456.
- [25] S. Shalev-Shwartz, S. Shammah, and A. Shashua. “Safe, multi-agent, reinforcement learning for autonomous driving”. In: *arXiv:1610.03295* (2016).
- [26] M. Zimmer et al. “Learning fair policies in decentralized cooperative multi-agent reinforcement learning”. In: *International Conference on Machine Learning*. PMLR. 2021, pp. 12967–12978.
- [27] J. Xiao et al. “Graph attention mechanism based reinforcement learning for multi-agent flocking control in communication-restricted environment”. In: *Information Sciences* 620 (2023), pp. 142–157.
- [28] J. Liu et al. “Deep Reinforcement Learning Task Assignment Based on Domain Knowledge”. In: *IEEE Access* 10 (2022), pp. 114402–114413.
- [29] J. Holder, N. Jaques, and M. Mesbahi. “Multi agent reinforcement learning for sequential satellite assignment problems”. In: *arXiv preprint arXiv:2412.15573* (2024).
- [30] M. Hutter. “Self-optimizing and Pareto-optimal policies in general environments based on Bayes-mixtures”. In: *International Conference on Computational Learning Theory*. Springer. 2002, pp. 364–379.

- [31] C. Tessler, D. J. Mankowitz, and S. Mannor. “Reward constrained policy optimization”. In: *arXiv preprint arXiv:1805.11074* (2018).
- [32] S. Paternain et al. “Constrained reinforcement learning has zero duality gap”. In: *Advances in Neural Information Processing Systems* 32 (2019).
- [33] M. Calvo-Fullana et al. “State augmented constrained reinforcement learning: Overcoming the limitations of learning with rewards”. In: *IEEE Transactions on Automatic Control* (2023).
- [34] S. Paternain et al. “Safe policies for reinforcement learning via primal-dual methods”. In: *IEEE Trans. on Aut. Control* 68.3 (2022), pp. 1321–1336.
- [35] L. Agorio et al. “Multi-agent assignment via state augmented reinforcement learning”. In: *arXiv preprint arXiv:2406.01782* (2024).
- [36] T. C. Aysal et al. “Broadcast gossip algorithms for consensus”. In: *IEEE Transactions on Signal processing* 57.7 (2009), pp. 2748–2761.
- [37] A. Casteigts et al. “Time-varying graphs and dynamic networks”. In: *Int. J. of Parallel, Emergent and Distributed Sys.* 27.5 (2012), pp. 387–408.
- [38] A. Nedić, A. Olshevsky, and W. Shi. “Achieving Geometric Convergence for Distributed Optimization Over Time-Varying Graphs”. In: *SIAM J. on Optimization* 27.4 (2017), pp. 2597–2633.
- [39] K. J. Arrow et al. *Studies in linear and non-linear programming*, Vol. 2. Stanford Univ. Press, 1958.
- [40] A. Nedić and A. Ozdaglar. “Subgradient methods for saddle-point problems”. In: *J. of optimization theory and applications* 142 (2009), pp. 205–228.
- [41] R. S. Sutton et al. “Policy gradient methods for reinforcement learning with function approximation”. In: *Adv. in neural info. proc. systems*. 2000, pp. 1057–1063.
- [42] J. M. Danskin. “The theory of max-min, with applications”. In: *SIAM Journal on Applied Mathematics* 14.4 (1966), pp. 641–664.
- [43] A. Dvoretzky. *On stochastic approximation*. Mathematics Division, Of. of Sci. Res., US Air Force, 1955.
- [44] R. G. Gallager. *Stochastic Processes: Theory for Applications*. Cambridge, UK: Cambridge Univ. Press, 2013.



**Leopoldo Agorio** received the B.Sc. degree in physics, and the B.Sc. and M.Sc. degrees in electrical engineering in 2018, 2019 and 2020 respectively, from the Universidad de la República (UdelaR) Montevideo, Uruguay. He is currently pursuing the Ph.D. degree at the University of Pittsburgh (Pitt), Pittsburgh, PA. He served as a teaching and research assistant at the Department of Applied Optics and the Department of Systems and Control at the School of Engineering, UdelaR, and at the Department

of Electrical and Computer Engineering at Pitt. His current research interests include mobile robotics, multi-agent reinforcement learning, graph signal processing and quantum computing. Leopoldo has also industry experience as an integrator engineer in electronics and robotics as well as applying computer vision technologies for quality control.



**Sean Van Alen** received the B.Sc. degree in Electrical and Computer Engineering from the University of Pittsburgh (Pitt) in May 2025. Sean received the 2024 Scholarship for Undergraduate Research from the department of Biomedical Engineering at Pitt, under the supervision of Dr. Bazerque.



**Santiago Paternain** received the B.Sc. degree in electrical engineering from Universidad de la República Oriental del Uruguay, Montevideo, Uruguay in 2012, the M.Sc. in Statistics from the Wharton School in 2018 and the Ph.D. in Electrical and Systems Engineering from the Department of Electrical and Systems Engineering, the University of Pennsylvania in 2018. He is currently an Assistant Professor in the Department of Electrical Computer and Systems Engineering at the Rensselaer Polytechnic Institute. Prior

to joining Rensselaer, Dr. Paternain was a postdoctoral Researcher at the University of Pennsylvania. His research interests lie at the intersection of machine learning and control of dynamical systems. Dr. Paternain was the recipient of the 2017 CDC Best Student Paper Award and the 2019 Joseph and Rosaline Wolfe Best Doctoral Dissertation Award from the Electrical and Systems Engineering Department at the University of Pennsylvania.



**Miguel Calvo-Fullana** received the B.Sc. degree in electrical engineering from the Universitat de les Illes Balears (UIB) in 2010 and the M.Sc. and Ph.D. degrees in electrical engineering from the Universitat Politècnica de Catalunya (UPC) in 2013 and 2017, respectively. He joined Universitat Pompeu Fabra (UPF) in 2023, where he is a Ramón y Cajal fellow. Prior to joining UPF, he held postdoctoral appointments at the University of Pennsylvania and the Massachusetts Institute of Technology, and during

his Ph.D., he was a research assistant at the Centre Tecnològic de Telecomunicacions de Catalunya (CTTC). His research interests lie in the broad areas of learning and optimization for autonomous systems, with a particular emphasis on multi-agent systems, wireless communication and networks connectivity. He is the recipient of best paper awards at ICC 2015, GlobalSIP 2015, and ICASSP 2020.



**Juan Andrés Bazerque** received a B.Sc. degree in electrical engineering from Universidad de la República (UdelaR), Montevideo, Uruguay, in 2003, and the M.Sc. and Ph.D. degrees in electrical engineering from the University of Minnesota (UofM), Minneapolis, in 2010 and 2013, respectively. After his Ph.D., he joined the Department of Electrical Engineering, UdelaR, as an Assistant Professor. In 2022, he joined the Department of Electrical and Computer Engineering at the University of Pittsburgh. In 2024,

he became Associate Editor for the Transactions on Signal Processing. His research interests include stochastic optimization and networked systems, focusing on reinforcement learning and algebraic signal processing. Dr. Bazerque was the recipient of the UofM’s Master Thesis Award 2009–2010, and a co-recipient of the best paper award at the 2nd International Conference on Cognitive Radio Oriented Wireless Networks and Communication in 2007.